Effects of rising CO_2 on the harmful cyanobacterium Microcystis

Sandrini, G.

Publication date
2016
Document Version
Final published version

Chapter 4

Strains of the harmful cyanobacterium *Microcystis aeruginosa* differ in gene expression and activity of inorganic carbon uptake systems at elevated CO_2 levels

Strains of the harmful cyanobacterium *Microcystis aeruginosa* differ in gene expression and activity of inorganic carbon uptake systems at elevated CO_2 levels

Giovanni Sandrini[1], Dennis Jakupovic[1], Hans C. P. Matthijs[1], Jef Huisman[1]

[1]*Department of Aquatic Microbiology, Institute for Biodiversity and Ecosystem Dynamics, University of Amsterdam, Amsterdam, The Netherlands*

Keywords: bicarbonate transport; CO_2-concentrating mechanism; climate change; harmful cyanobacteria; *Microcystis aeruginosa*; natural selection

This chapter is published as:
Sandrini G, Jakupovic D, Matthijs HCP, Huisman J. (2015). Strains of the harmful cyanobacterium *Microcystis aeruginosa* differ in gene expression and activity of inorganic carbon uptake systems at elevated CO_2 levels. *Applied and Environmental Microbiology* **81:** 7730–7739.

Abstract

Cyanobacteria are generally assumed to be effective competitors at low CO_2 levels because of their efficient CO_2-concentrating mechanism (CCM), yet how bloom-forming cyanobacteria will respond to rising CO_2 concentrations is less clear. Here, we investigate changes in CCM gene expression at ambient CO_2 (400 ppm) and elevated CO_2 (1100 ppm) in six strains of the harmful cyanobacterium *Microcystis*. All strains downregulated *cmpA* encoding the high-affinity bicarbonate uptake system BCT1 at elevated CO_2, whereas both the low- and high-affinity CO_2 uptake genes were expressed constitutively. Four strains downregulated the bicarbonate uptake genes *bicA* and/or *sbtA*, whereas two strains showed constitutive expression of the *bicA-sbtA* operon. In one of the latter strains, a transposon insert in *bicA* caused low *bicA* and *sbtA* transcript levels, which made this strain solely dependent on BCT1 for bicarbonate uptake. Activity measurements of the inorganic carbon (C_i) uptake systems confirmed the CCM gene expression results. Interestingly, genes encoding the RuBisCO enzyme, structural carboxysome components and carbonic anhydrases were not regulated. Hence, *Microcystis* mainly regulates the initial uptake of inorganic carbon, which might be an effective strategy for a species experiencing strongly fluctuating C_i concentrations. Our results show that CCM gene regulation of *Microcystis* differs among strains. The observed genetic and phenotypic variation in CCM responses may offer an important template for natural selection, leading to major changes in the genetic composition of harmful cyanobacterial blooms at elevated CO_2.

Introduction

CO_2 concentrations in the atmosphere may double during this century (IPCC 2014). In marine ecosystems, enhanced dissolution of atmospheric CO_2 causes ocean acidification (Orr *et al.*, 2005; Doney *et al.*, 2009). In freshwaters, however, CO_2 concentrations may vary widely. In many lakes, the dissolved CO_2 concentration exceeds the concentration expected from equilibrium with the atmosphere, due to the input of large amounts of organic carbon from terrestrial systems (Cole *et al.*, 1994; Sobek *et al.*, 2005). Conversely, the photosynthetic activity of dense phytoplankton blooms can deplete the CO_2 concentration far below atmospheric levels, which increases pH and makes bicarbonate the most abundant inorganic carbon species (Talling, 1976; Balmer and Downing, 2011; Verspagen *et al.*, 2014b). Cyanobacteria are often considered to be very successful competitors at low CO_2 levels (Shapiro, 1997; Low-Décarie *et al.*, 2011), and global warming is predicted to favor an expansion of cyanobacterial blooms in eutrophic waters (Paerl and Huisman, 2008; Davis *et al.*, 2009; O'Neil *et al.*, 2012). However, the response of bloom-forming cyanobacteria to elevated CO_2 levels is not yet well understood.

Cyanobacteria typically use a CO_2-concentrating mechanism (CCM) with up to five different uptake systems for inorganic carbon (C_i): three for bicarbonate and two for CO_2 uptake (Price, 2011). The two sodium-dependent bicarbonate uptake systems, BicA and SbtA, are present in some but not all freshwater cyanobacteria (Price *et al.*, 2004; Rae *et al.*, 2011; Sandrini *et al.*, 2014). BicA combines a low affinity for bicarbonate with a high flux rate, whereas SbtA usually has a high affinity for bicarbonate but a low flux rate (Price *et al.*, 2004; Du *et al.*, 2014). Hence, BicA operates more effectively at high bicarbonate concentrations and *vice versa* SbtA at low bicarbonate concentrations (Price *et al.*, 2004; Sandrini *et al.*, 2014). The third bicarbonate system, BCT1, is present in most freshwater cyanobacteria, and resembles SbtA with a high affinity for bicarbonate and a low flux rate. However, in contrast to SbtA, BCT1 does not require sodium and is directly ATP-dependent (Omata *et al.*, 1999). The two CO_2 uptake systems, NDH-I_3 and NDH-I_4, are also present in most freshwater cyanobacteria, and convert the passively diffusing CO_2 inside the cell into bicarbonate via NADPH-driven electron flow (Maeda *et al.*, 2002). NDH-I_3 combines a high affinity for CO_2 with a low flux rate, whereas NDH-I_4 combines a low affinity with a high flux rate (Maeda *et al.*, 2002; Price *et al.*, 2002). Inside the cyanobacterial cells, bicarbonate accumulates in the cytoplasm and then diffuses into the carboxysomes, where it is converted back to CO_2 via carbonic anhydrases to enable efficient carbon fixation by RuBisCO (Price, 2011).

Microcystis is a harmful cyanobacterium that forms dense blooms in lakes all over the world (Verspagen *et al.*, 2006; Qin *et al.*, 2010; Mickalak *et al.*, 2013). Moreover, many strains are capable of producing microcystin, which is a powerful hepatotoxin for birds, mammals and humans (Jochimsen *et al.*, 1998; Huisman *et al.*, 2005). Recently, it was shown that *Microcystis* strains show considerable genetic diversity in their C_i uptake genes (Sandrini *et al.*, 2014). Some strains lack the *sbtA* gene (genotype I), other strains lack *bicA* (genotype II), and again others contain the genes for all five C_i uptake systems (genotype III). Some strains also acquired transposon inserts in the *bicA-sbtA* operon (Sandrini *et al.*, 2014), but it is unknown if this affects expression of *bicA* and *sbtA* in these strains. Although expression of the CCM genes has been extensively studied in the model cyanobacterium *Synechocystis* PCC 6803 (Omata *et al.*, 2001; McGinn *et al.*, 2003; Wang *et al.*, 2004; Eisenhut *et al.*, 2007), CCM gene expression patterns of the environmentally relevant cyanobacterium *Microcystis* have attracted only recent interest (Penn *et al.*, 2014; Sandrini *et al.*, 2015a; Steffen *et al.*, 2015).

In this study, we compare expression of the C_i uptake genes in response to changing CO_2 conditions among *Microcystis* strains representative of the different C_i uptake genotypes. Studies with *Synechocystis* PCC 6803 showed that genes for the high-affinity uptake systems for CO_2 (NDH-I_3) and bicarbonate (SbtA and BCT1) are induced at low CO_2, whereas expression of low-affinity C_i uptake systems (BicA and NDH-I_4) remains unaltered (Wang *et al.*, 2004;

Eisenhut *et al.*, 2007). It seems likely that the same expression patterns apply to *Microcystis*, although the presence of different C_i uptake genotypes could lead to variation in gene expression among *Microcystis* strains. We therefore defined two hypotheses for our study: (1) high-affinity C_i uptake genes are downregulated at elevated CO_2 (1100 ppm), whereas (2) low-affinity C_i uptake genes are expressed constitutively in *Microcystis*. To investigate these hypotheses, we compared the CCM gene expression of six *Microcystis* strains at ambient and elevated CO_2 levels. Furthermore, we measured O_2 evolution of the strains exposed to different C_i conditions to compare the activity of their C_i uptake systems. The results reveal an unexpected diversity of CO_2 responses within the genus *Microcystis*.

Materials and Methods

Microcystis strains

We studied six *Microcystis* strains with different C_i uptake systems (**Figure 4.1**). The C_i uptake genotypes of these strains were described in a previous study (Sandrini *et al.*, 2014). Strain PCC 7806 contains the *bicA* gene but lacks the *sbtA* gene, and belongs to C_i uptake genotype I. Strains NIES-843 and CCAP 1450/11 contain the *sbtA* gene but lack a complete *bicA* gene, and hence belong to genotype II. Strain NIVA-CYA 140 combines *sbtA* with a complete *bicA* gene that is no longer functional because of a transposon insert, and therefore this strain was also assigned to genotype II. Strains HUB 5-3 and PCC 7005 contain both the *bicA* and *sbtA* genes in the same operon, and are therefore assigned to genotype III (**Figure 4.1**). The four genes encoding the high-affinity bicarbonate transporter BCT1 (*cmpABCD*) as well as the genes encoding the high-affinity CO_2 uptake system NDH-I_3 (*chpY*, *ndhD3*, *ndhF3* and other *ndh* genes) and the low-affinity CO_2 uptake system NDH-I_4 (*chpX*, *ndhD4*, *ndhF4* and other *ndh* genes) were present in all six strains (Sandrini *et al.*, 2014). Moreover, genome-wide microarray analysis showed that *Microcystis* PCC 7806 expresses all its CCM genes (Sandrini *et al.*, 2015a).

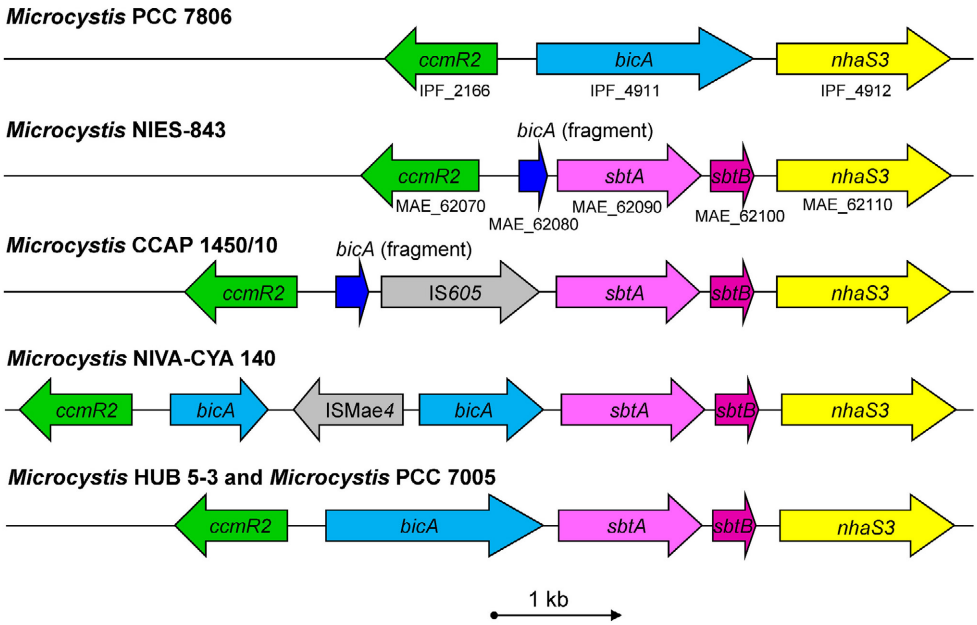

Figure 4.1. The *bicA-sbtA* operon of the six *Microcystis* strains of this study. Gene *ccmR2* encodes a LysR transcriptional regulator that most likely regulates the expression of the *bicA-sbtA* operon. Some strains contain a complete *bicA* gene, whereas others only contain a small fragment. The grey arrows (IS*605* and ISMae*4*) indicate transposon inserts. Gene *sbtB* encodes a protein that regulates the activity of SbtA (Du *et al.*, 2014). Gene *nhaS3* encodes a proton/sodium antiporter. The IPF numbers are the locus tags of PCC 7806, and the MAE numbers are the locus tags of NIES-843. The protein sequence identity between the *Microcystis* strains is 99% for BicA and 97-99% for SbtA.

Experimental set-up

We used the exponential phase of batch culture experiments exposed to ambient pCO_2 (400 ppm) and elevated pCO_2 (1100 ppm) in the gas flow to study gene expression and activity of the C_i uptake systems.

First, the six *Microcystis* strains were precultured in 1 L Erlenmeyer flasks in modified BG11 medium (Rippka *et al.*, 1979; with 10 mmol L^{-1} $NaNO_3$ and no added Na_2CO_3/$NaHCO_3$) for one week. The precultures were incubated at 25°C with 400 ppm of pCO_2 and at 120 rpm in an orbital shaker incubator (Gallenkamp, Leicester, UK), with light provided by TL-D 30W/33-640 white fluorescent tubes (Philips, Eindhoven, the Netherlands) at 20 µmol photons m^{-2} s^{-1}. Microscopy checks did not reveal any contaminations.

Subsequently, new 1 L Erlenmeyer flasks with 400 mL modified BG11 medium were inoculated with the exponentially growing pre-cultures at an OD_{750} of ~0.080. Four biological replicates were used for each strain. The Erlenmeyer flasks were topped with foam stoppers to allow gas exchange and placed in an Infors HT Multritron Pro incubator (Infors Benelux,

Doetinchem, the Netherlands) at 25°C, 400 ppm pCO_2 and shaken at 120 rpm. Light was provided by white fluorescent tubes (Gro-lux F36W/Gro-T8; Havells-Sylvania Germany GmbH, Erlangen, Germany). It was recently shown that microcystins can bind to RuBisCO during oxidative stress (Zilliges *et al.*, 2011), which may affect CO_2 fixation. Therefore, we decided to use low light levels of 20 µmol photons m^{-2} s^{-1}during the batch culture experiments, to minimize possible effects of microcystins on carbon fixation. After two days at 400 ppm, the pCO_2 in the incubator was increased to 1100 ppm. The pCO_2 concentration in the gas mixture was checked regularly with an Environmental Gas Monitor for CO_2 (EGM-4; PP Systems, Amesbury, MA, USA). The flasks were sampled on a daily basis, and after four days the experiment was ended.

pH, DIC and cell counts

The pH was measured immediately after sampling with a Lab 860 pH meter in combination with a BlueLine 28 Gel pH electrode (SCHOTT Instruments GmbH, Mainz, Germany).

To determine the concentrations of dissolved inorganic carbon (DIC), culture samples were immediately pelleted (5 min at 4,000 *g* and 20°C). Supernatant was filtered over 0.45 µm pore size 47 mm polyethersulfone membrane filters (Sartorius AG, Goettingen, Germany). The filtrate was transferred to sterile plastic urine analysis tubes (VF-109SURI; Terumo Europe N.V., Leuven, Belgium), which were filled completely (using a needle to leave all air out), and stored at 4°C until analysis. A TOC-V_{CPH} TOC analyzer (Shimadzu, Kyoto, Japan) was used to determine DIC (measured three- to five-fold per sample). DIC concentrations were converted to CO_2(aq), bicarbonate and carbonate concentrations using the measured pH of the samples (Stumm and Morgan, 1996).

Cell numbers and biovolumes of samples from the different cultures were determined in triplicate using a Casy 1 TTC cell counter with a 60 µm capillary (Schärfe System GmbH, Reutlingen, Germany). Because the strains differed in cell size, we report the cyanobacterial abundances as biovolumes.

RNA extraction

Just before and 20 h after increasing pCO_2 from 400 to 1100 ppm, 40 mL samples were taken for reverse transcription-quantitative PCR (RT-qPCR) analysis, immediately cooled on ice and centrifuged for 5 minutes at 4,000 *g* and 4°C in a pre-cooled centrifuge. The pellets were immediately resuspended in 1 mL TRIzol (Life Technologies, Grand Island, NY, USA), frozen in liquid nitrogen and stored at -80°C. Subsequent RNA extraction and purification was done as described before (Sandrini *et al.*, 2015a). RNA concentrations were quantified using a

Nanodrop 1000 spectrophotometer (Thermo Scientific, San Jose, CA, USA), and all RNA samples had A_{260}/A_{280} and A_{260}/A_{230} values above 1.8.

RT-qPCR analysis

We investigated the expression of CCM genes using primers designed in this and previous studies (Sandrini *et al.*, 2014, 2015a) (**Table S4.1, Supplementary Information**). The transcripts of the following CCM genes were targeted: *cmpA* (encoding a subunit of the high-affinity bicarbonate transporter BCT1), *bicA* and *sbtA* (the two sodium-dependent bicarbonate transporters), *chpX* (hydration subunit of the low-affinity CO_2 uptake system NDH-I_4), *chpY* (hydration subunit of the high-affinity CO_2 uptake system NDH-I_3), *ccmR* and *ccmR2* (two CCM transcriptional regulators), *rbcX* (chaperone for RuBisCO), *ccmM* (structural component of the carboxysomes), *ccaA1* and *ccaA2* (two carboxysomal carbonic anhydrases), and *ecaA* (periplasmic carbonic anhydrase). In addition, we targeted transcripts of the 16S rRNA gene and *mcyB* gene (microcystin synthetase).

Reverse transcription reactions were done as described previously (Sandrini *et al.*, 2015a), using Superscript III (Life Technologies, Grand Island, NY, USA). Subsequently, the qPCR Maxima® SYBR Green Master Mix (2x) (Thermo Fisher Scientific, Pittsburgh, PA, USA) was applied with our primers to the obtained cDNA samples as described before (Sandrini *et al.*, 2015a), to analyze PCR amplification in a ABI 7500 Real-Time PCR device (Applied Biosystems, Foster City, CA, USA). The two-step cycling protocol was used, with a denaturation temperature of 95°C (15 s) and a combined annealing/extension temperature of 60°C (60 s) during 40 cycles. Melting curve analysis was performed on all measured samples to rule out non-specific PCR products. ROX solution (passive reference dye) was used to correct for any well-to-well variation.

We calculated relative changes in gene expression after 20 h of elevated pCO_2 using the 16S rRNA gene as reference gene. The LinRegPCR software tool version 2012.3 (Ramakers *et al.*, 2003; Ruijter *et al.*, 2009) was used for baseline correction, calculation of quantification cycle (*Cq*) values and calculation of the amplification efficiency (*E*) of each individual run using linear regression (**Table S4.1, Supplementary Information**). Amplification efficiencies of individual samples were between 1.8 and 2.0. Relative changes in gene expression were calculated with the comparative C_T method (Livak and Schmittgen, 2001).

One-tailed *t*-tests were applied to identify significant changes in gene expression (n = 4 biological replicates), using the false discovery rate (FDR) to correct for multi-hypothesis testing (Benjamini *et al.*, 2001). FDR adjusted p-values < 0.05 combined with log2 expression changes of < -0.8 or > 0.8 were considered significant.

O_2 evolution experiments

We studied the activity of different C_i uptake systems of *Microcystis* strains acclimated to low or high CO_2 levels using O_2 measurements with an Oxy-4 mini O_2 optode (PreSens GmbH, Regensburg, Germany). In mineral medium without nitrate, the initial O_2 evolution rate reflects the C_i uptake rate of cyanobacteria (Sandrini *et al.*, 2015a; Miller *et al.*, 1988). Cells acclimated to low CO_2 levels were obtained from batch cultures exposed to 400 ppm pCO_2 for four days. As a result, the C_i availability of the mineral medium was low, CO_2(aq) was depleted to 0.0018±0.0004 µmol L^{-1} and the bicarbonate concentration was 76±10 µmol L^{-1} (**Figure S4.1, Supplementary Information**). Cells acclimated to high CO_2 levels were obtained from batch cultures exposed to 400 ppm pCO_2 for two days, and subsequently to 1100 ppm pCO_2 for two days. The C_i availability in these cultures was high, CO_2(aq) was 4.2±1.3 µmol L^{-1} and the bicarbonate concentration 1062±43 µmol L^{-1} (**Figure S4.1, Supplementary Information**).

Samples from these batch cultures were pelleted (4,000 *g* for 5 min at 20°C), washed 1x and then resuspended in C_i-deplete and N-deplete modified BG11 medium (no added $NaCO_3$/$NaHCO_3$ and $NaNO_3$, but with added 0.1 mmol L^{-1} NaCl and 10 mmol L^{-1} CAPSO-KOH pH 9.8). The medium was aerated with N_2 gas before usage. The response of the cells was studied at pH 9.8, to mimic dense blooms in which bicarbonate is the dominant C_i species. The OD_{750} of washed and resuspended samples was 0.300, and 3 mL of these samples was inserted into custom-made double walled glass incubation chambers equipped with sensors connected to the O_2 optode device. The glass chambers were connected to a RM6 water bath (Lauda, Postfach, Germany) to keep the temperature of the samples constant at 20.3°C. Magnetic stirring was used for mixing. The O_2 optode sensors were calibrated with N_2 gas (0% oxygen) and pressurized air (21% oxygen). A saturating amount of light was provided by KL1500 compact Schott lamps (Schott AG, Mainz, Germany). Saturating light levels lead to high O_2 evolution rates, which facilitate detection of differences between the treatments. In pilot experiments, we found that the photosynthetic rates (expressed per chlorophyll *a* [chl *a*]) of strains PCC 7806 and PCC 7005 were saturated at ~400 µmol photons m^{-2} s^{-1}, and did not decrease up to 1,000 µmol photons m^{-2} s^{-1}. Therefore, we used an incident light intensity (I_{in}) = 500 µmol photons m^{-2} s^{-1} for the O_2 evolution experiments.

At the start of the experiments, cells were allowed to take up all remaining C_i in the incubation chambers, which was monitored by a gradual decrease of the O_2 evolution. Subsequently, the rate of O_2 evolution (mg L^{-1} min^{-1}) was measured during 15 min intervals in a control treatment without additions and after adding 20, 300 or 10,000 µmol L^{-1} of $KHCO_3$ in the presence of different concentrations of NaCl and LiCl (**Table 4.1**). The different bicarbonate concentrations stimulate different C_i uptake systems. Sodium ions were added to stimulate the sodium-dependent bicarbonate transporters BicA and SbtA, whereas lithium ions

were added to block bicarbonate uptake. In total, we applied six different treatments, which each activated or suppressed one or more different C_i uptake systems (**Table 4.1**). The units were converted to µmol O_2 · mg^{-1} chl *a* · min^{-1} using data from chlorophyll *a* measurements that were acquired with HPLC as described previously (Sandrini *et al.*, 2015a). For each strain acclimated at low or high pCO_2 levels, we tested if O_2 evolution rates were different between the treatments using one-way analysis of variance with *post hoc* comparison of the means based on Tukey's HSD test (α = 0.05; n = 4 per treatment).

Table 4.1. Treatments in the O_2 evolution experiments, to study activity of the different C_i uptake systems.

Treatment			Dissolved inorganic carbon		Active C_i uptake system(s)
$KHCO_3$ (µmol L^{-1})	NaCl (mmol L^{-1})	LiCl (mmol L^{-1})	CO_2(aq) (µmol L^{-1})	HCO_3^- (µmol L^{-1})	
0	0.1	0	0	0	None (control)
20	0.1	0	0.006	15.80	BCT1
20	25	0	0.006	15.80	BCT1, SbtA
300	25	0	0.090	236.7	BCT1, SbtA, BicA
300	25	25	0.090	236.7	None
10,000	25	25	3.000	7891	NDH-I_3, NDH-I_4

Different concentrations of $KHCO_3^-$, NaCl and LiCl were added to induce or block the activity of specific C_i uptake systems. The resulting CO_2(aq) and HCO_3^- concentrations expected at pH 9.8 and 20.3°C are shown. The last column indicates which C_i uptake systems are mostly active at the applied conditions.

Results

Changes in DIC and pH at elevated CO_2

Six *Microcystis* strains (PCC 7806, NIES-843; CCAP 1450/10; NIVA-CYA 140; HUB 5-3 and PCC 7005) with different C_i uptake systems were grown at atmospheric pCO_2 conditions of 400 ppm (**Figure 4.2**). Assuming equilibrium with this atmospheric pressure, one would expect a CO_2(aq) concentration of 13.5 µmol L^{-1}, and the pH of the mineral medium without cells would be ~7. However, owing to the photosynthetic activity of the *Microcystis* population, the CO_2(aq) concentration was depleted to <0.1 µmol L^{-1}, the bicarbonate concentration was <330 µmol L^{-1}, and the pH increased to 10-11 depending on the strain (**Figures 4.2 and 4.3**). After two days, we raised the pCO_2 in the gas flow to 1100 ppm. As a consequence, the CO_2(aq) concentration increased to 1-12 µmol L^{-1} depending on the strain, the bicarbonate concentration increased to 800-1500 µmol L^{-1}, and the pH dropped 1-2 units (**Figures 4.2 and 4.3**).

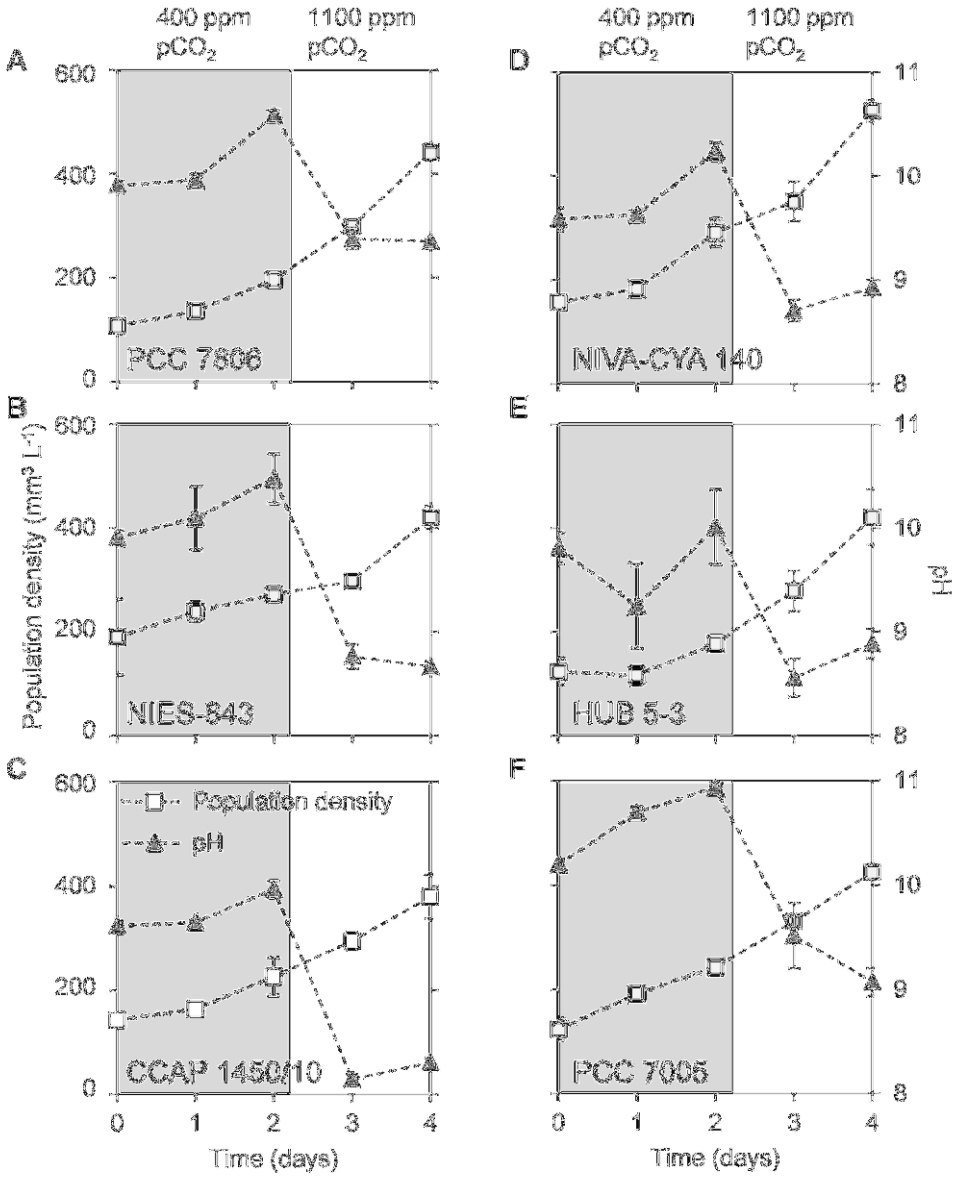

Figure 4.2. Growth and pH during the exponential phase in batch cultures of six *Microcystis* strains. (A) PCC 7806. **(B)** NIES-843. **(C)** CCAP 1450/10. **(D)** NIVA-CYA 140. **(E)** HUB 5-3. **(F)** PCC 7005. The batch cultures were exposed to 400 ppm pCO_2 in the gas flow for two days (shaded area), and thereafter the pCO_2 concentration was increased to 1100 ppm (non-shaded area). The mineral medium contained 10 mmol L^{-1} sodium ions. Error bars indicate standard deviation (n = 4 biological replicates).

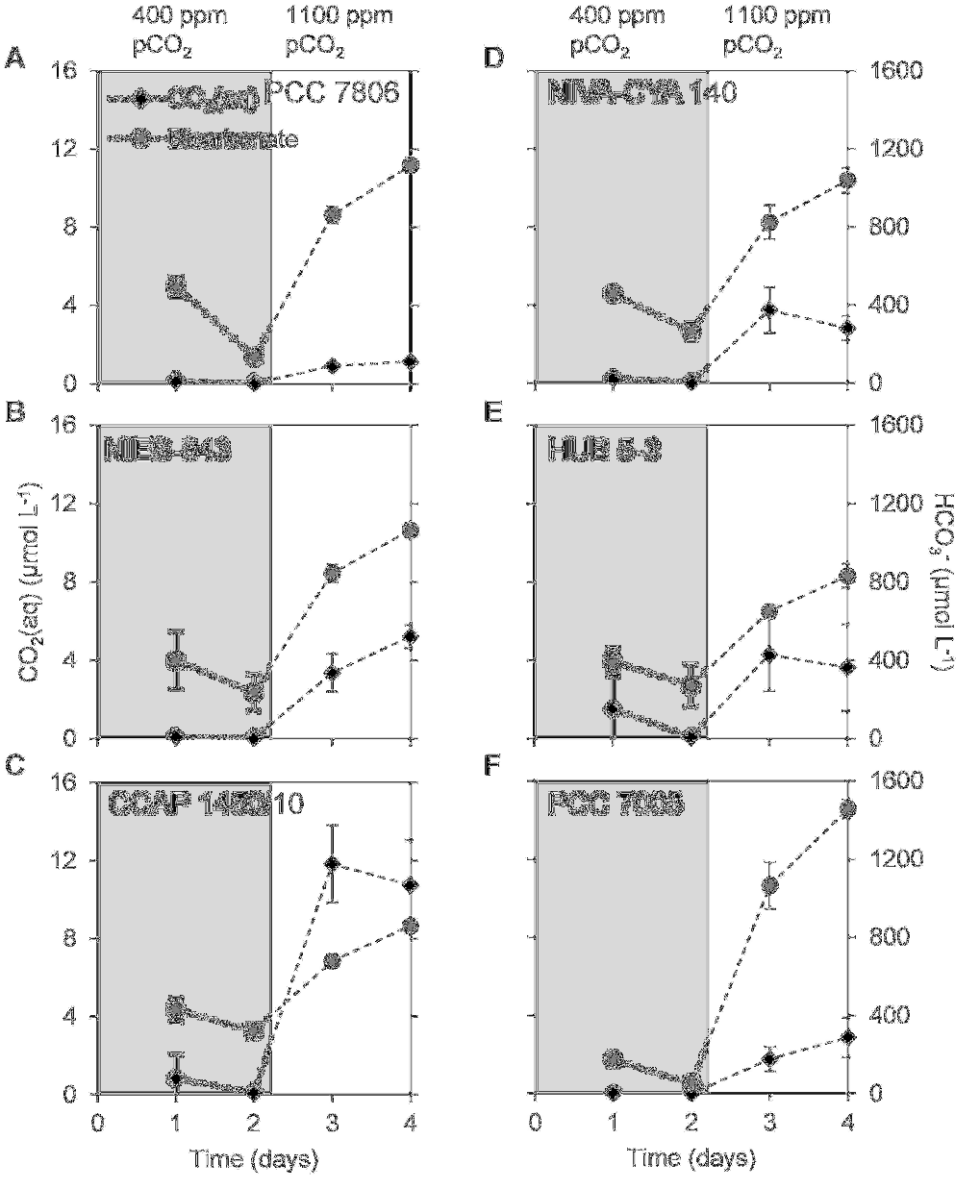

Figure 4.3. Dissolved CO_2 and bicarbonate concentration during the exponential phase in batch cultures of six *Microcystis* strains. (A) PCC 7806. **(B)** NIES-843. **(C)** CCAP 1450/10. **(D)** NIVA-CYA 140. **(E)** HUB 5-3. **(F)** PCC 7005. The batch cultures were exposed to 400 ppm pCO_2 in the gas flow for two days (shaded area), and thereafter the pCO_2 concentration was increased to 1100 ppm (non-shaded area). The mineral medium contained 10 mmol L^{-1} sodium ions. Error bars indicate standard deviation (n = 4 biological replicates).

Changes in gene expression at elevated CO_2

Expression of selected CCM genes was monitored before and 20 h after increasing the pCO_2 in the gas flow (**Figure 4.4 and Table S4.2, Supplementary Information**). At elevated pCO_2, all strains showed significant downregulation of *cmpA*, although four strains (PCC 7806, CCAP 1450/10, NIVA-CYA 140, PCC 7005) showed a stronger downregulation than two others (NIES-843 and HUB 5-3). The *sbtA* gene encoding for the high-affinity bicarbonate transporter SbtA was significantly downregulated in strains NIES-843, CCAP 1450/10 and HUB 5-3, but was constitutively expressed in strains NIVA-CYA 140 and PCC 7005. The *bicA* gene encoding for the low-affinity bicarbonate transporter BicA was downregulated in strains PCC 7806 and HUB 5-3, but was also constitutively expressed in strains NIVA-CYA 140 and PCC 7005. None of the six strains showed significant changes in gene expression of the CO_2 uptake genes *chpX* and *chpY* (**Figure 4.4**).

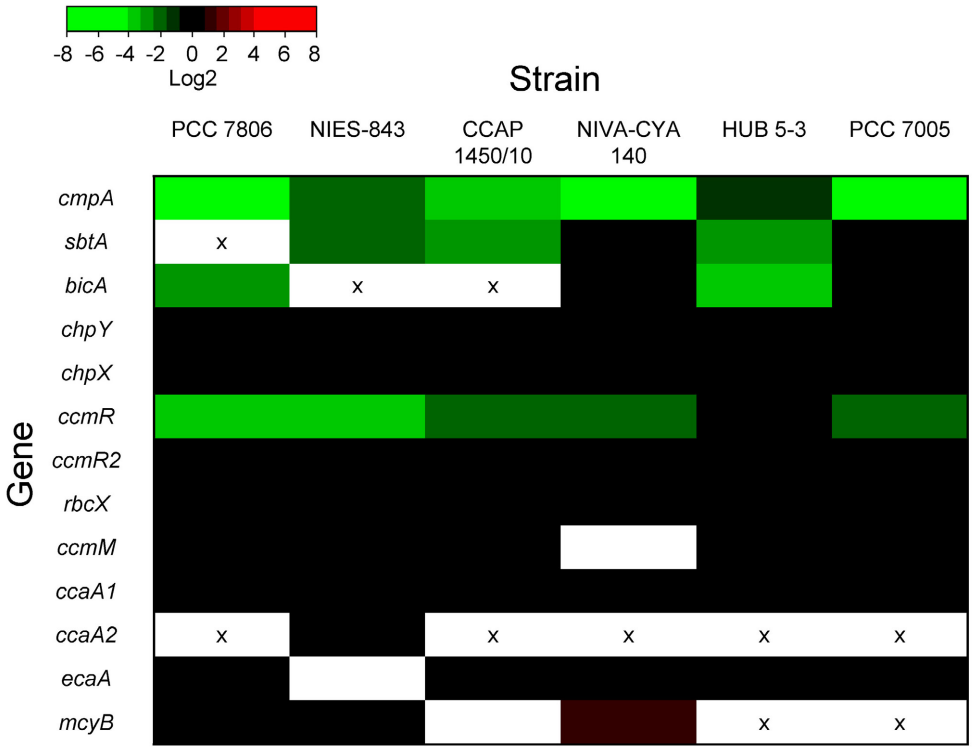

Figure 4.4. Heatmap of changes in gene expression at elevated CO_2 for each of the six *Microcystis* strains. Gene expression changes were obtained by RT-qPCR applied to samples taken before and 20 h after increasing the pCO_2 level from 400 to 1100 ppm. The color bar indicates log2 values. Significant downregulated genes are shown in green, significant upregulated genes are shown in red, and non-significant changes ($p > 0.05$) or log2 values between -0.8 and 0.8 are shown in black. Genes not measured are shown in white and genes absent in strains are marked with 'x'. The detailed RT-qPCR results are presented in Table S4.2, Supplementary Information.

Expression of the CCM transcriptional regulator *ccmR* was reduced significantly at elevated CO_2 in all strains, except strain HUB 5-3. In contrast, expression of the additional transcriptional regulator *ccmR2* located upstream of the *bicA-sbtA* operon of *Microcystis* did not change significantly in any of the strains. Expression of several other CCM genes (*rbcX*, *ccmM*, *ccaA1*, *ccaA2* and *ecaA*) was also not affected by elevated CO_2 in any of the strains.

Expression of *mcyB* was unaltered in PCC 7806 and NIES-843, and increased slightly but significantly in NIVA-CYA 140.

C_i uptake activity of low- and high-CO_2 acclimated cells

We studied O_2 evolution of the *Microcystis* strains to compare the activity of their C_i uptake systems when the strains were acclimated to low or high CO_2 conditions (**Figure 4.5**). We applied six different treatments to activate different C_i uptake systems, as explained in **Table 4.1**. For the interpretation of these results, we note that the response of the O_2 evolution rates to the treatments can be compared within each strain at a given pCO_2 level (*i.e.*, within the panels of **Figure 4.5**), but cannot be compared quantitatively among the strains or among the two different pCO_2 levels (*i.e.*, among the panels of **Figure 4.5**). The reason is that other factors also influence the O_2 evolution rates, for example, the pigment concentrations and amounts of PSI and PSII may differ between strains and can also change with elevated CO_2 (Sandrini *et al.*, 2015a). The results can be compared among strains in a relative sense, for example two different strains can show a significant increase in O_2 evolution after addition of 20 µmol L^{-1} $KHCO_3$, while a third strain does not. The O_2 evolution rates of strain NIES-843 were highly variable among the biological replicates and declined strongly after two hours. Repetition of the O_2 evolution experiments with this strain did not improve the results, indicating that NIES-843 could not withstand the incubation conditions. Therefore, we only report the results for the other five *Microcystis* strains.

For cells acclimated to low C_i conditions, addition of 20 µmol L^{-1} $KHCO_3$ in the presence of only 0.1 mmol L^{-1} NaCl induced significantly more O_2 production than the control for all strains, except for strain HUB 5-3 which showed a non-significant response (**Figure 4.5A-E**). This result indicates that BCT1 was active in all strains, although its activity was low in strain HUB 5-3. Application of 20 µmol L^{-1} $KHCO_3$ and 25 mmol L^{-1} NaCl led to a significantly higher O_2 production than at 20 µmol L^{-1} $KHCO_3$ and 0.1 mmol L^{-1} NaCl for strains PCC 7806, CCAP 1450/10 and HUB 5-3. This result indicates that in response to the added sodium ions these three strains activated their sodium-dependent bicarbonate transporter SbtA. However, strain PCC 7806 does not have SbtA, and its response might indicate activation of the other sodium-dependent bicarbonate transporter BicA. The O_2 production at 300 µmol L^{-1} $KHCO_3$ and 25 mmol L^{-1} NaCl was not significantly higher than

at 20 µmol L^{-1} $KHCO_3$ and 25 mmol L^{-1} NaCl for any of the strains. This result indicates that cells acclimated to low C_i conditions relied largely on the high-affinity transporters BCT1 and SbtA for their bicarbonate uptake. Subsequent addition of 25 mmol L^{-1} LiCl (in the presence of 300 µmol L^{-1} $KHCO_3$ and 25 mmol L^{-1} NaCl) blocked bicarbonate uptake, and as a consequence O_2 production of all strains was reduced to similar levels as the control treatment. Finally, addition of 10,000 µmol L^{-1} $KHCO_3$ in the presence of 25 mmol L^{-1} LiCl and 25 mmol L^{-1} NaCl strongly increased the CO_2(aq) concentration in the medium (**Table S4.1, Supplementary Information**) and restored O_2 production in all strains (**Figure 4.5A-E**). Since lithium still blocked bicarbonate uptake, this result indicates that CO_2 uptake was active in all strains.

For cells acclimated to high C_i conditions, addition of 20 µmol L^{-1} $KHCO_3$ in the presence of only 0.1 mmol L^{-1} NaCl induced significantly more O_2 production than the control only for strain PCC 7005 (**Figure 4.5F-J**). This result indicates that the high-affinity bicarbonate transporter BCT1 was hardly active in any of the strains acclimated to high C_i conditions, except strain PCC 7005. Application of 20 µmol L^{-1} $KHCO_3$ and 25 mmol L^{-1} NaCl led to a significantly higher O_2 production than at 0.1 mmol L^{-1} NaCl for strains PCC 7806, HUB 5-3 and PCC 7005, indicating that these strains activated their sodium-dependent bicarbonate transporter SbtA. Strain PCC 7806 does not have SbtA, and its response might indicate activation of the other sodium-dependent bicarbonate transporter BicA. The O_2 production at 300 µmol L^{-1} $KHCO_3$ and 25 mmol L^{-1} NaCl was significantly higher than at 20 µmol L^{-1} $KHCO_3$ and 25 mmol L^{-1} NaCl for strains PCC 7806 and HUB 5-3, indicating that their low-affinity but high-flux bicarbonate transporter BicA was active when cells were acclimated to high C_i conditions. Subsequent addition of 25 mmol L^{-1} LiCl blocked bicarbonate uptake, and as a consequence O_2 production of all strains was reduced to similar levels as the control treatment. Finally, addition of 10,000 µmol L^{-1} $KHCO_3$ in the presence of 25 mmol L^{-1} LiCl and 25 mmol L^{-1} NaCl increased O_2 production in comparison to the control (**Figure 4.5F-J**), indicating that CO_2 uptake was active in all strains.

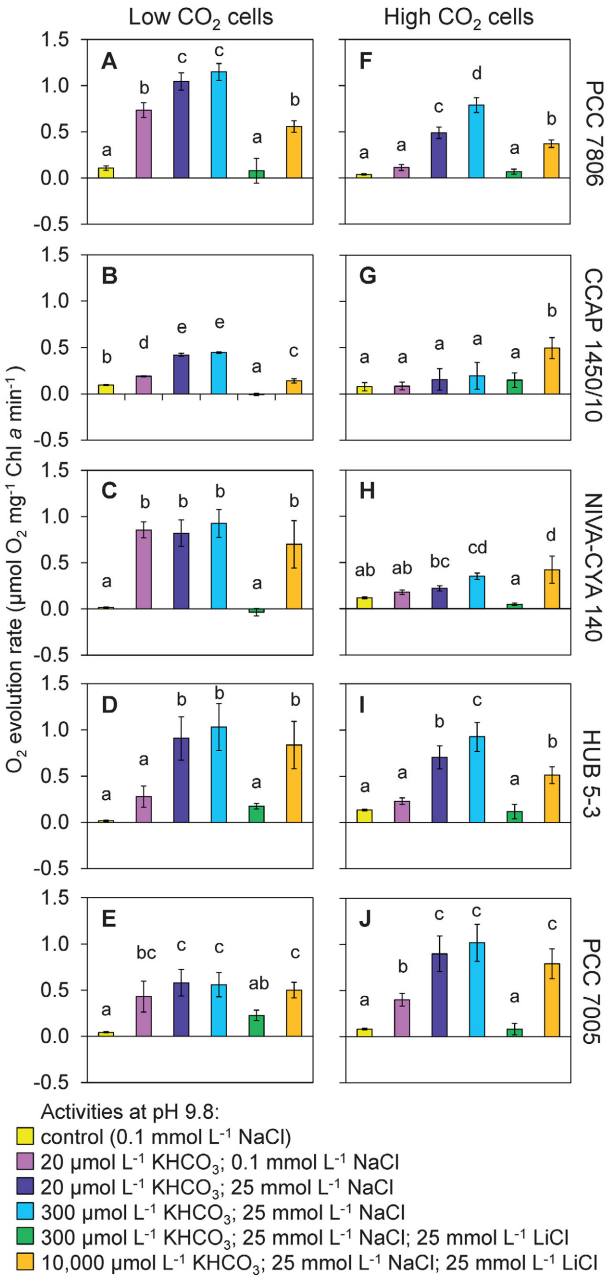

Figure 4.5. Activity of C_i uptake systems of five *Microcystis* strains, inferred from O_2 evolution. The strains were acclimated to either **(A-E)** low CO_2 levels, or **(F-J)** high CO_2 levels. O_2 evolution was measured after addition of different concentrations of $KHCO_3$, NaCl and LiCl to induce or block the activity of specific C_i uptake systems, as indicated in Table 4.1. Error bars indicate standard deviation (n = 4 biological replicates per treatment). Different letters above the bars indicate significant differences between the treatments, as tested by one-way analysis of variance with *post hoc* comparison of the means based on Tukey's HSD test (α = 0.05).

Discussion

Evaluation of hypotheses

Our results enable evaluation of the hypotheses that (1) high-affinity C_i uptake genes of *Microcystis* are downregulated at elevated CO_2 (1100 ppm), whereas (2) low-affinity but high-flux C_i-uptake genes are constitutively expressed. Consistent with the first hypothesis, our results show that the *cmpA* gene encoding the bicarbonate-binding subunit of the high-affinity bicarbonate transporter BCT1 was downregulated in all strains. Down-regulation of BCT1 at elevated CO_2 could potentially be cost effective for the cells, because bicarbonate uptake by BCT1 is expected to require 1 ATP molecule per molecule of bicarbonate (**Table 4.2**). However, the other high-affinity bicarbonate uptake gene, *sbtA*, was downregulated at elevated CO_2 in only three of the five *sbtA*-containing strains. Furthermore, the gene *chpY* encoding the hydration subunit of the high-affinity CO_2 uptake system NDH-I_3 was not down-regulated at elevated CO_2 in any of the strains. Hence, the first hypothesis applies to *cmpA* (BCT1) and partly to *sbtA* of the two high-affinity bicarbonate uptake systems, but does not apply to *chpY* of the high-affinity CO_2 uptake system.

Consistent with the second hypothesis, the gene *chpX* encoding the hydration subunit of the low-affinity CO_2 uptake system NDH-I_4 was constitutively expressed in all strains. However, the low-affinity bicarbonate uptake gene, *bicA*, was constitutively expressed only in strains NIVA-CYA 140 (where it is not functional because of a transposon insert; **Figure 4.1**) and PCC 7005, but was downregulated at elevated CO_2 in strains PCC 7806 and HUB 5-3. Hence, the second hypothesis is supported by *chpX* (NDH-I_4), whereas the low-affinity bicarbonate uptake gene *bicA* shows a more variable response.

General observations

Given that both hypotheses received only partial support, what general observations can still be obtained from the gene expression patterns of the *Microcystis* strains? First, it is noteworthy that several C_i uptake systems and one of their transcriptional regulators were regulated in response to elevated CO_2, whereas other important CCM genes encoding the enzyme RuBisCO, structural components of the carboxysome and carbonic anhydrases were not regulated at all (**Figure 4.4**). Furthermore, a recent transcriptome study of *Microcystis* PCC 7806 found that expression of the *ppc* gene, encoding phosphoenolpyruvate (PEP) carboxylase involved in an alternative C_i assimilation pathway, also remained constant at elevated CO_2 conditions (Supplementary Table 4 in Sandrini *et al.*, 2015a). These results indicate that the CCM genes of *Microcystis* respond to elevated CO_2 mainly at the very first steps of the carbon fixation process, by regulating the initial acquisition of inorganic carbon. *Microcystis* is a buoyant cyanobacterium that can develop dense blooms in eutrophic lakes, where it will be exposed to

large fluctuations in CO_2 availability at both daily and seasonal time scales (Maberly, 1996). A highly specific response that mainly adjusts the initial C_i uptake systems, without large changes in expression of the carboxysome genes and genes of the downstream carbon assimilation pathways, could preserve energy and offer a robust strategy for a species that often experiences strongly fluctuating C_i conditions (Sandrini *et al.*, 2015a).

Second, all C_i uptake genes investigated in this study were either downregulated or remained unchanged at elevated CO_2; none of them were upregulated. Hence, all C_i uptake systems that a strain was capable to produce, were available for the cells at low CO_2 levels, including the low-affinity C_i uptake systems. Third, the genes *chpX* and *chpY* of both CO_2 uptake systems were expressed constitutively, which might again be an adaptation to fluctuating CO_2 conditions. Constitutive expression of the high-affinity CO_2 uptake system NDH-I_3 might also be an adaptation to intercept low intracellular concentrations of CO_2 leaking from the carboxysomes.

Methodological aspects

Previously, the cellular response of strain PCC 7806 to elevated CO_2 was investigated in highly-controlled chemostats using whole-genome microarrays (Sandrini *et al.*, 2015a). In the present study we simplified the experimental set-up to batch cultures and limited our analysis to a smaller set of genes using RT-qPCR, which enabled investigation of a larger number of strains. We included strain PCC 7806 in our present study, to check the consistency of the results.

Strain PCC 7806 downregulated expression of *cmpA* and *bicA* at elevated CO_2 in both the previous and the present study (**Figure 4.4**). Furthermore, both studies showed constitutive expression of the CO_2 uptake, carboxysomal and RuBisCO genes and downregulation of the transcriptional regulator gene *ccmR*, although *ccmR2* was only downregulated in the previous study (Sandrini *et al.*, 2015a). Moreover, the O_2 evolution data of PCC 7806 show that BCT1 and BicA were both active at low pCO_2 conditions (**Figure 4.5A**), whereas BicA but not BCT1 was active at high pCO_2 conditions (**Figure 4.5F**), in agreement with the previous study (Sandrini *et al.*, 2015a). Hence, the results of both studies are in good agreement, which gives confidence in the applied methods.

In our O_2 evolution experiments, the cells were exposed to different salt treatments (**Table 4.1**). This could potentially bias the results, because *Microcystis* strains differ in their salt tolerance and potassium ion sensitivity (Sandrini *et al.*, 2015b). In particular, strain PCC 7005 is very sensitive to elevated potassium ion concentrations and lacks several salt tolerance genes, whereas strain PCC 7806 is much more tolerant to potassium ions and can withstand 170 mmol L^{-1} NaCl (Tonk *et al.*, 2007; Sandrini *et al.*, 2015b). We therefore tried to minimize salt

stress, by exposing the cells to the different treatments for only 15 min. The results show that even the salt- and potassium-sensitive strain PCC 7005 maintained high O_2 evolution rates in the treatment with the highest salinity (10 mmol L^{-1} $KHCO_3$, 25 mmol L^{-1} LiCl and 25 mmol L^{-1} NaCl; **Figure 4.5**), and hence the applied salinities apparently did not hinder the activity of the cells during this short time interval.

Expression and activity of the sodium-dependent C_i uptake genes

Expression of the sodium-dependent bicarbonate uptake genes *bicA* and *sbtA* varied widely among the strains. Even similar genotypes, such as strains HUB 5-3 and PCC 7005 that both belong to genotype III (*bicA*+*sbtA*), showed contrasting expression patterns for their bicarbonate uptake genes (**Figure 4.4**). These two strains have *bicA* and *sbtA* located in one operon (Sandrini *et al.*, 2015a), and hence co-transcription explains why the expression patterns of these two genes are coupled (**Figure 4.4**). The O_2 evolution data indicate that HUB 5-3 mainly relies on its sodium-dependent bicarbonate uptake systems at low C_i conditions (**Figure 4.5D**), whereas PCC 7005 mainly relies on ATP-dependent bicarbonate uptake by BCT1 (**Figure 4.5E**). Hence, a reduction of the cellular investments in bicarbonate uptake at elevated CO_2 would be most effective by downregulation of the *bicA-sbtA* operon for HUB 5-3 and by down-regulation of BCT1 for PCC 7005, in line with the observed changes in gene expression (**Figure 4.4**).

Strain NIVA-CYA 140 contains *sbtA* but has a transposon insert in the middle of a complete *bicA* gene (**Figure 4.1**), and was therefore assigned to C_i uptake genotype II (no *bicA*) (Sandrini *et al.*, 2015a). At low pCO_2 the transcription level of *sbtA* (relative to 16S rRNA) was ~45x lower in this strain than in the other strains, indicating that the transposon insert interfered with transcription of the *bicA-sbtA* operon. Indeed, the strain depended strongly on BCT1 at low pCO_2 conditions, as evidenced from lack of stimulation by added sodium ions in the O_2 evolution experiments (**Figure 4.5C**), whereas the strain depended mainly on CO_2 uptake at high pCO_2 conditions (**Figure 4.5H**). Hence, most likely this strain does not use the sodium-dependent bicarbonate uptake systems BicA and SbtA, and therefore has a phenotype that deviates from all other *Microcystis* strains.

Strain CCAP 1450/10 also has a transposon insert, located between a small *bicA* fragment and a complete *sbtA* gene (**Figure 4.1**). Yet, the gene expression results (**Figure 4.4**) and the O_2 evolution data (**Figure 4.5B**) show that the transposon insert did not hinder expression of *sbtA* in this strain.

Comparison of CCM gene regulation of *Microcystis* with other cyanobacteria

Previously, the CCM genes of the model cyanobacteria *Synechocystis* PCC 6803, *Synechococcus* PCC 7002 and *Synechococcus* 7942 were studied in detail (Omata *et al.*, 1999; Ohkawa *et al.*, 2000; Omata *et al.*, 2001; Shibata *et al.*, 2002; McGinn *et al.*, 2003; Woodger *et al.*, 2003; Price *et al.*, 2004; Wang *et al.*, 2004; Eisenhut *et al.*, 2007; Schwarz *et al.*, 2011; Burnap *et al.*, 2015). Comparison of the CCM genes of our *Microcystis* strains with these model cyanobacteria reveals several similarities and differences (**Tables 4.2 and 4.3**).

In all cyanobacteria investigated thus far, genes encoding the ATP-dependent high-affinity bicarbonate transporter BCT1 are induced at low C_i conditions, whereas genes encoding the low-affinity CO_2 uptake system NDH-I_4 are constitutively expressed (**Table 4.2**). Hence, our two hypotheses do apply to the genes of these two uptake systems. The constitutive expression of genes encoding the high-affinity CO_2 uptake system NDH-I_3 in all *Microcystis* strains and the high-affinity bicarbonate transporter SbtA in some *Microcystis* strains deviates from the induction of these genes in the other three cyanobacteria. The presence and expression of *bicA* appears quite variable, not only in *Microcystis* but also in other cyanobacteria.

The CCM transcriptional regulators also differ among the cyanobacteria (**Table 4.3**). CcmR can regulate transcription of several C_i uptake genes. In *Synechocystis* PCC 6803, CcmR appeared to be a repressor of *sbtA* and the high-affinity CO_2 operon, but not of *bicA* (Wang *et al.*, 2004; Schwarz *et al.*, 2011). In contrast, in *Synechococcus* PCC 7002, CcmR appeared to be a repressor of *bicA* and *sbtA*, and possibly the high-affinity CO_2 uptake operon (Woodger *et al.*, 2007; Burnap *et al.*, 2015). In *Microcystis*, CcmR probably regulates expression of the *cmpABCD* operon (encoding for BCT1), since downregulation of *ccmR* at elevated pCO_2 coincided with downregulation of the *cmpA* gene (**Figure 4.4**). *Synechocystis* PCC 6803 and *Synechococcus* PCC 7942 use another transcriptional regulator, CmpR, for the *cmpABCD* operon (Omata *et al.*, 2001; Schwarz *et al.*, 2011), which is absent from *Microcystis*. CcmR2 is the most likely transcriptional regulator for the *bicA* and *sbtA* genes in *Microcystis*, given the location of *ccmR2* upstream of the *bicA-sbtA* operon (Sandrini *et al.*, 2014).

Table 4.2. Gene expression of the five different C_i uptake systems in *Microcystis* and three model cyanobacteria.

C_i uptake system (genes involved)	Energy cost[a]	Gene expression[b]			
		Microcystis strains*	*Synechocystis* PCC 6803*	*Synechococcus* PCC 7002#	*Synechococcus* PCC 7942*
BCT1 (*cmpABCD*)	1 ATP per HCO_3^-	Inducible under low pCO_2	Inducible under low pCO_2	–	Inducible under low pCO_2
SbtA (*sbtA*)	0.5 ATP per HCO_3^-	Constitutively expressed/ inducible under low pCO_2 / –	Inducible under low pCO_2	Inducible under low pCO_2	Inducible under low pCO_2
BicA (*bicA*)	0.25 ATP per HCO_3^-	Constitutively expressed/ inducible under low pCO_2 / –	Constitutively expressed	Inducible under low pCO_2	–
NDH-I_3 (*chpY* and others)	1 NADPH per CO_2 to HCO_3^- conversion	Constitutively expressed	Inducible under low pCO_2	Inducible under low pCO_2	Inducible under low pCO_2
NDH-I_4 (*chpX* and others)	1 NADPH per CO_2 to HCO_3^- conversion	Constitutively expressed	Constitutively expressed	Constitutively expressed	Constitutively expressed
References[c]	(Price *et al.*, 2002, 2011a; McGrath and Long, 2014)	This study	(Wang *et al.*, 2004; Eisenhut *et al.*, 2007)	(Woodger *et al.*, 2007)	(Woodger *et al.*, 2003; Schwarz *et al.*, 2011)

[a]The estimated energy costs of the different C_i uptake systems are indicated in terms of molecules of ATP or NADPH per molecule CO_2 or HCO_3^-.

[b]The *Microcystis* strains, *Synechocystis* PCC 6803 and *Synechococcus* PCC 7942 originate from freshwater (brackish water for *Microcystis* PCC 7806); *Synechococcus* PCC 7002 has a marine origin. A dash (–) indicates that the C_i uptake system is absent.

[c]The source or reference(s)are indicated in the bottem row for each column of data.

Table 4.3. Presence and function of CCM transcriptional regulators in *Microcystis* and three model cyanobacteria.

Transcriptional regulator	Location in genome	Function[a]			
		Microcystis	*Synechocystis* PCC 6803	*Synechococcus* PCC 7002	*Synechococcus* PCC 7942
CcmR	Upstream of high-affinity CO_2 uptake operon	Repressor/ activator of *cmpABCD* operon (BCT1)	Repressor of *sbtA* and high-affinity CO_2 operon (not *bicA*)	Repressor of *sbtA* and *bicA* (possibly of high-affinity CO_2 operon)	–
CcmR2	Upstream of *bicA-sbtA* operon	Repressor/ activator of *bicA*/*sbtA* operon	–	–	–
CmpR	Upstream of *cmpABCD* operon (BCT1) or separate location	–	Activator of *cmpABCD* operon	–	Activator of *cmpABCD* operon (possibly repressor of *sbtA* and high-affinity CO_2 operon)
References[b]		This study and (Sandrini *et al.*, 2014)	(Figge *et al.*, 2001; Wang *et al.*, 2004;)	(Woodger *et al.*, 2007)	(Woodger *et al.*, 2003; Price *et al.*, 2008)

[a]A dash (–) indicates that the transcriptional regulator is absent.

[b]The source or reference(s) are indicated in the bottem row for each column of data.

Ecological implications

In conclusion, our results reveal an unexpected diversity in CO_2 responses of cyanobacteria. It was already known that *Microcystis* strains differ in their C_i uptake genes, which promotes variation in their CO_2 response (Sandrini *et al.*, 2014). Our results show that, on top of this genotypic diversity, there is also considerable phenotypic variation because strains with the same C_i uptake genes can show contrasting expression patterns and may differ widely in the activity of their C_i uptake systems. In other words, cyanobacterial strains differ in their adaptation to changing CO_2 conditions not only because of variation in genetic composition but also because of further variation at the transcriptional and physiological level.

It is often argued that cyanobacteria generally have a very effective CCM, and are therefore particularly strong competitors at low CO_2 levels in comparison to eukaryotic phytoplankton (Shapiro, 1997). However, we know now that there is major variation in the CCM tactics among cyanobacteria, and even among different strains within the same genus. Some *Microcystis* strains perform well at low CO_2, whereas other strains are much better

competitors under high CO_2 conditions (Sandrini *et al.*, 2014; Van de Waal *et al.*, 2011). This genetic and phenotypic variation in C_i uptake systems provides cyanobacterial communities with the potential for rapid adaptation and acclimation to changing CO_2 conditions. These differential responses also indicate that the ongoing rise in atmospheric CO_2 concentrations is likely to be more beneficial for some cyanobacterial strains than for others, which may lead to major changes in the genetic composition of harmful cyanobacterial blooms.

Acknowledgements

We are most grateful to the reviewers for their helpful comments. This research was supported by the Division of Earth and Life Sciences (ALW) of the Netherlands Organization for Scientific Research (NWO). We declare that we have no conflict of interest related to the manuscript.

Supplementary Information

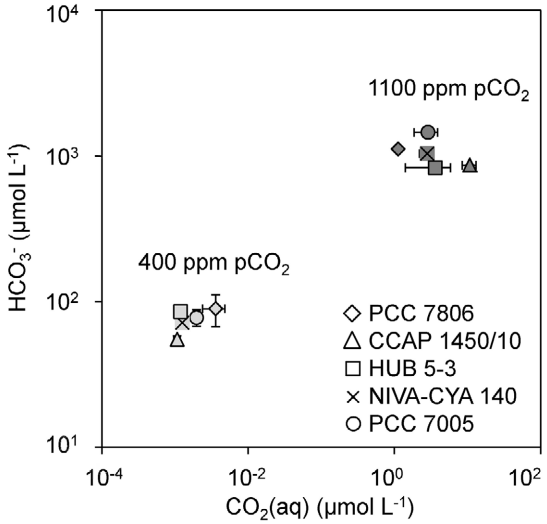

Figure S4.1. Dissolved CO_2 (CO_2(aq)) and bicarbonate concentrations in batch cultures of *Microcystis* strains exposed to ambient pCO_2 (400 ppm; light grey symbols) or elevated pCO_2 (1100 ppm; dark grey symbols) in the gas flow. CO_2(aq) and bicarbonate concentrations were determined after four days of culturing. Error bars indicate standard deviation (n = 4).

Table S4.1. *Microcystis* primers used in this study for RT-qPCR gene expression analyses.

Primer name	Sequence 5'→ 3' (length)	Gene symbol	Function of complete protein/complex	Locus tag[a]	Accession no. (Genbank)	Expected product size (bp)	Amplification efficiency (*E*)[b]	Reference
16SrRNA-F	GTCGAACGGGAATCT TCGGAT (21)	*16S rRNA*	Used here as reference gene for quantification of gene expression	*IPF_5548*	AM778951.1	157	1.91±0.07	Sandrini *et al.*, 2015a
16SrRNA-R	GCTAATCAGACGCAA GCTCTTC (22)							Sandrini *et al.*, 2015a
cmpA-F	GTTAAACACCCAGGG TAACGGA (22)	*cmpA*	High-affinity ATP-dependent bicarbonate uptake system	*IPF_2181*	AM778958.1	180	1.86±0.02	Sandrini *et al.*, 2015a
cmpA-R	GCTAACCAGTAACGA ATCCAGAAGT (25)							Sandrini *et al.*, 2015a
sbtA-F	CTGGCCTTTTTGATT GGTGG (20)	*sbtA*	High-affinity bicarbonate/sodium symporter	*MAE_62090*	AP009552.1	143	1.87±0.02	This study
sbtA-R	AGGTTGGAATTGCGG ATGG (19)							This study
bicA-F	CAAGCTAACGGTCGC ATCAT (20)	*bicA*	Low-affinity bicarbonate/sodium symporter	*IPF_4911*	AM778949.1	132	1.88±0.02	Sandrini *et al.*, 2015a
bicA-R	AGGCACATCACTCAA GTCCA (20)							Sandrini *et al.*, 2015a
chpX-F	CCTGTCAAGTCCTCC TCTCAT (21)	*chpX*	Low-affinity CO_2 uptake system	*IPF_1842*	AM778957.1	113	1.88±0.02	Sandrini *et al.*, 2015a
chpX-R	TTCAGGATACCCACT ACCTCG (21)							Sandrini *et al.*, 2015a
chpY-F	ATATCGCCAAAATGC CGACC (20)	*chpY*	High-affinity CO_2 uptake system	*IPF_1545*	AM778958.1	114	1.80±0.04	Sandrini *et al.*, 2014
chpY-R	GACATCATCCGCACC TGTTC (20)							Sandrini *et al.*, 2014
ccmR-F	CCTACCGTCTCAACC CAAGT (20)	*ccmR*	Transcriptional regulator of CCM genes	*IPF_1549*	AM778958.1	109	1.88±0.02	Sandrini *et al.*, 2014
ccmR-R	ACAGTAATTCCTGAC CCGCTT (21)							Sandrini *et al.*, 2014
ccmR2-F	TCCTTGGGATAAACC ACATACCA (23)	*ccmR2*	Transcriptional regulator of CCM genes	*IPF_2166*	AM778949.1	204	1.86±0.02	Sandrini *et al.*, 2014
ccmR2-R	TTTTCTCGACCATGG CATCAC (21)							Sandrini *et al.*, 2014
rbcX-F	CGGATCATGACGGTA AGAGAACA (23)	*rbcX*	RuBisCO chaperone, in operon with RuBisCO L/S subunit genes	*IPF_2531*	AM778933.1	157	1.86±0.01	Sandrini *et al.*, 2015a
rbcX-R	ATTCCGATGTCTCTG GTTGACT (22)							Sandrini *et al.*, 2015a
ccmM-F	AAGTCCACACCTTCT CTAACCTC (23)	*ccmM*	Carboxysome structural protein	*IPF_5695*	AM778933.1	118	1.87±0.02	Sandrini *et al.*, 2014
ccmM-R	CTGTCGTCGCCAATG TGAA (19)							Sandrini *et al.*, 2014
ccaA1-F	ACTCCTGCGGTTAAT ACTGTGG (22)	*ccaA*	Carboxysome carbonic anhydrase	*IPF_5538*	AM778919.1	97	1.88±0.02	Sandrini *et al.*, 2014
ccaA1-R	GATAAATGCGATCAG CTTGGGAG (23)							Sandrini *et al.*, 2014
ccaA2-F	ATTCGTTCCCGATTA CATCAAGG (23)	*ccaA2*	Carboxysome carbonic anhydrase	*MAE_36560*	AP009552.1	137	1.88±0.02	Sandrini *et al.*, 2014
ccaA2-R	AAGTTGCTCAACGGG ATCG (19)							Sandrini *et al.*, 2014
ecaA-F	CCCAAGAACCTTCTC CTGAAATG (23)	*ecaA*	α-type carbonic anhydrase; presumably mainly present in the periplasmic space	*IPF_4566*	AM778932.1	187	1.86±0.02	Sandrini *et al.*, 2014
ecaA-R	GCCAATTGTTGCAGT TGTTGG (21)							Sandrini *et al.*, 2014
mcyB-F	ATCCCATGCTCAGAG ACGTT (20)	*mcyB*	Microcystin synthesis	*IPF_375*	AM778952.1	163	1.86±0.03	Sandrini *et al.*, 2014
mcyB-R	AGATGTCCGCAGGGA TTCAT (20)							Sandrini *et al.*, 2014

[a]The locus tags are from *Microcystis* PCC 7806 (IPF) and *Microcystis* NIES-843 (MAE).

[b]The amplification efficiency *E* for the individual primers sets was based on 32-48 amplification curves, except for *ccaA2* that was based on only 8 curves.

Table S4.2. Changes in gene expression at elevated CO_2 for each of the six *Microcystis* strains.

Microcystis strain	Gene	Log2 relative gene expression change	Standard deviation	FDR adjusted *p*-values
PCC 7806	*cmpA*	**-6.998**	1.456	**0.011**
	bicA	**-3.093**	0.407	**0.007**
	chpX	0.132	0.097	0.130
	chpY	-0.101	0.205	0.458
	ccmR	**-3.778**	0.548	**0.007**
	ccmR2	-0.436	0.079	**0.010**
	rbcX	0.062	0.509	0.848
	ccmM	-0.244	0.204	0.168
	ccaA1	0.144	0.091	0.104
	ecaA	-0.367	0.046	**0.007**
	mcyB	-0.276	0.107	**0.040**
NIES-843	*cmpA*	**-1.713**	0.486	**0.022**
	sbtA	**-1.818**	0.273	**0.007**
	chpX	0.154	0.261	0.412
	chpY	0.575	0.607	0.254
	ccmR	**-3.683**	0.377	**0.007**
	ccmR2	-0.393	0.256	0.109
	rbcX	**0.839**	0.369	0.052
	ccmM	0.642	0.387	0.096
	ccaA1	0.246	0.178	0.462
	ccaA2	-0.169	0.284	0.412
	mcyB	0.758	0.539	0.127
CCAP 1450/10	*cmpA*	**-3.830**	0.171	**0.007**
	sbtA	**-2.870**	0.590	**0.011**
	chpX	-0.036	0.483	0.906
	chpY	0.026	0.541	0.930
	ccmR	**-2.165**	0.428	**0.011**
	ccmR2	-0.695	0.369	0.072
	rbcX	0.399	0.051	**0.007**
	ccmM	0.041	0.304	0.843
	ccaA1	-0.279	0.485	0.414
	ecaA	-0.253	0.402	0.399
	mcyB	-0.252	0.415	0.411
NIVA-CYA 140	*cmpA*	**-7.225**	0.348	**0.002**
	sbtA	-0.432	0.766	0.417
	bicA	0.274	0.198	0.127
	chpX	-0.366	0.373	0.246
	chpY	0.111	0.229	0.459
	ccmR	**-1.837**	0.291	**0.007**
	ccmR2	-0.370	0.704	0.444
	rbcX	-0.712	0.318	0.053
	ccaA1	-0.482	0.733	0.399
	ecaA	0.094	0.144	0.399
	mcyB	**0.966**	0.290	**0.023**

Table S4.2 continued.

HUB 5-3	*cmpA*	**-1.169**	0.433	**0.037**
	sbtA	**-2.703**	0.619	**0.013**
	bicA	**-3.235**	0.775	**0.014**
	chpX	-0.162	0.414	0.530
	chpY	-0.390	0.446	0.271
	ccmR	**-1.425**	0.723	0.068
	ccmR2	**-0.820**	0.552	0.114
	rbcX	0.221	0.111	0.068
	ccmM	0.092	0.247	0.542
	ccaA1	-0.310	0.356	0.271
	ecaA	-0.458	0.511	0.269
PCC 7005	*cmpA*	**-4.328**	0.600	**0.007**
	sbtA	0.518	0.489	0.124
	bicA	0.591	0.202	**0.031**
	chpX	0.346	0.177	0.068
	chpY	0.123	0.301	0.521
	ccmR	**-1.635**	0.349	**0.011**
	ccmR2	0.369	0.395	0.254
	rbcX	-0.612	0.956	0.399
	ccmM	-0.513	0.768	0.399
	ccaA1	0.306	0.123	**0.043**
	ecaA	0.519	0.155	**0.023**

Gene expression changes were obtained by RT-qPCR applied to samples taken before and 20 h after increasing the pCO_2 level from 400 to 1100 ppm. Bold values in the 'Log2 relative gene expression' column indicate expression changes < -0.8 or > 0.8. Bold values in the 'FDR adjusted *p*-values' column indicate significant changes ($p < 0.05$).